



HME coupled with FDM 3D printing of a customized oral solid form to treat pediatric epilepsy

M. Monteil^a, N.M. Sanchez-Ballester^{a,b}, A. Aubert^a, O. Gimello^a, S. Begu^{a,*}, I. Soulairol^{a,b,*}

^a ICGM, Univ Montpellier, CNRS, ENSCM, Montpellier, France

^b Department of Pharmacy, Nîmes University Hospital, Nîmes, France

ARTICLE INFO

Keywords:

HME
FDM
Sodium valproate
Pediatric
3D printing

ABSTRACT

Interest in hot-melt extrusion (HME) and fused deposition material (FDM) printing has increased in recent years, for the production of tailored medications for patients with specific requirements, such as pediatrics. Liquid forms are often preferred for children but these forms are less stable than oral solid forms (such as tablets or powder), requiring preservative not always suitable for children. Then, the aim of this study is to develop a dose-adapted dispersible 3D printed forms using HME with FDM to treat pediatric epilepsy. Polyethylene oxide (PEO)-based 3D printed forms were developed with sodium valproate (VAL) as model drug at different concentrations. The effects of polyethylene glycol (PEG)'s molecular weight (PEG6K and PEG35K) used as plasticizer on the formulations' mechanical, thermal and rheological properties were investigated. Formulation with 10 % (w/w) of VAL were printed with PEG6K and PEG35K, while only PEG35K was suitable for extruding and printing a formulation containing 30 % (w/w) of VAL due to its rheological properties. Steric exclusion chromatography coupled with refraction index was used to quantify VAL content, indicating uniform concentration in the filament after extrusion. Dissolution test in acidic media display over 80 % of VAL released within 20 to 25 min, reaching the Eur. Ph. Criteria of a rapid release. The outcomes of this study present suitable formulations to produce personalized dispersible form using HME with FDM 3D printing to treat pediatric epilepsy (1 month to 4 years old patients with dosage from 18 to 247 mg/kg/day) for the treatment of epilepsy.

1. Introduction

Among the different routes of drug administration, oral administration is often preferred due to its convenience and cost-effectiveness. Tablets represent more than 50 % of all marketed solid oral pharmaceutical preparations as they are easier and more economical to develop, manufacture, transport and store than liquid forms (Kotsybar et al., 2023). However, they are less suitable for patients with swallowability issues, such as pediatric and geriatric populations and come with specific dosage, hard to adapt to patient's weight, which is mandatory for children. Epilepsy, is the most frequent chronic neurologic disease affecting pediatric patients (Aaberg et al., 2017) widely treat with sodium valproate (VAL), a first-generation antiepileptic. Due to its poor solubility and high permeability sodium valproate (VAL) is a Class II drug in the biopharmaceutical classification system (Chang, 1979). Epilepsy treatment requires high flexibility with a daily dose of 10 to 30 mg/kg per day divided in 1 to 3 intakes ("Easyprep Pédiatrie"; Depakine 200 mg/ml, 2024). Due to the quick increase of patients' weight in the

first months of life, the treatment must be flexible to provide a dose adapted. As the dose is usually divided in 2 doses per day, a 1-month old child (3,6 kg) medicated with 10 mg/kg requires 18 mg per intake, while a 4-years old (16.2 kg) child medicated with 30 mg/kg requires 243 mg per take (WHO, 2022). With these specifications, solids forms are limited while liquid formulations offer more dose flexibility. However, liquid forms require the use of conservatives for stability issues and involve higher transport and packaging costs (Mfoafo et al., 2021). 3D printing (3DP) is a technology that can meet all the requirements of solid and liquid forms with great dosing flexibility, the development of dispersible forms to ease the administration and storage. Among the various 3D printing techniques, fused deposition modeling (FDM) stands out due to its cost-effectiveness, absence of post-processing steps, and solvent-free composition (Cailleaux et al., 2021). FDM 3D printed filaments are prepared using hot melt extrusion (HME), widely used in the pharmaceutical field to produce solid dispersions. Nonetheless, HME coupled with FDM raises challenges with risks of drug's thermal degradation. To prevent this, polymer with low melting point and

* Corresponding authors at: ICGM, Univ Montpellier, CNRS, ENSCM, Montpellier, France (I. Soulairol).

E-mail addresses: Sylvie.begu@umontpellier.fr (S. Begu), Ian.soulairol@umontpellier.fr (I. Soulairol).

<https://doi.org/10.1016/j.ijpharm.2025.125345>

Received 28 October 2024; Received in revised form 10 February 2025; Accepted 11 February 2025

Available online 12 February 2025

0378-5173/© 2025 The Authors. Published by Elsevier B.V. This is an open access article under the CC BY license (<http://creativecommons.org/licenses/by/4.0/>).

plasticizer properties such as Polyethylene glycols (PEG) can be used (Hoffmann et al., 2022; Xu et al., 2020). PEG, marketed over a wide range of molecular weights, are often used in pharmaceuticals formulations as viscosity modifiers. They are classified as PEGs when molecular weight is below 100 K g/mol, while those with higher molecular weights are classified as polyethylene oxides (PEOs) (Ma et al., 2014).

The aim of this study is to formulate an FDM-printed oral solid form and, considering the targeted population, the printed forms must be dispersible in water before administration. PEO 100 K g/mol was selected as polymer carrier due to its low processing temperature (60 – 100 °C), water solubility and good processability in HME and FDM (Baird et al., 2010; Melocchi et al., 2016). PEGs were used as plasticizers to improve processability of the formulation. While several studies have investigated the effect of the polymeric carrier molecular weight on FDM printed forms, few studies focused on the influence of the plasticizer's length, hence, formulations with PEG 6 K g/mol (PEG6K) and PEG 35 K g/mol (PEG35K) were prepared (Cantin et al., 2016; Isreb et al., 2019). The formulations were characterized by XRPD, TGA and DSC to investigate the effect of HME and FDM printing on the physico-chemical properties of VAL, PEO and PEGs. As the flowing property is a key parameter in HME and FDM printing, a rheological study was performed to determine the influence of PEGs' molecular weight and VAL loading on the formulation's viscosity. Then, filament's flexural modulus was determined using three-point bend test to assess their flexibility. Considering the need of dose flexibility, the drug load of the formulation, as well as the height and infill density of the printed forms were varied. Due to the pediatric targeted population, the resulting printed forms must be dispersed in water before administration in solution. Hence, disintegration tests were performed in water. Then, the dissolution profiles of VAL were determined in gastric media to mimic oral administration. Finally, a 3-months stability study was performed on filaments and printed forms stored at room temperature and a relative humidity of 40 %.

2. Materials and Methods

2.1. Materials

Polyethylene glycol 35 K g/mol (PEG35K), 6 K g/mol (PEG6K) and polyethylene oxide 100 K g/mol (PEO), sodium valproate (VAL) salt 99 % purity, sodium chloride, 0.1 mol/l hydrochloric acid (HCl) and acetonitrile HPLC-grade were purchased from Sigma-Aldrich. For analysis, ultrapure water was produced by a Synergy® UV water system (Millipore SA, Molsheim, France). All solvents were of analytical grade, unless otherwise specified.

2.2. Hot-melt extrusion

For each formulation, 10 g of powder mixture were prepared. PEO, PEG35K, PEG6K and sodium valproate were weighted using a Sartorius balance (Sartorius Lab Instrument GmbH & Co. KG Goettingen, Germany) and mixed using a Heidolph Reax 2 overhead mixer. Filaments were extruded at 70 °C and 50 rpm using a Pharma Mini HME equipped with a conical co-rotating twin-screw extruder with a rod-shaped aluminum die ($\varnothing = 1.75$ mm) (Thermo Fisher Scientific, Karlsruhe, Germany), a gravimetric feeder and a force feeder (Thermo Fisher Scientific, Karlsruhe, Germany). This device enables the powder to be continuously drawn into the extruder at a controlled flow rate of 0.1 kg/h. Filaments' diameter was adjusted using a M22 transport conveyor and measured using a diameter monitor laser system (Thermo Fisher Scientific, Karlsruhe, Germany). After each HME, the filaments were stored as a spool at room temperature in a Drybox ADL-3D77, EurekaDryTech (ERM Automatisme, Carpentras, France), at a relative humidity (RH) of 40 % before being used for further analysis. The temperature and humidity in the extrusion laboratory were monitored using a Traceable® hygrometer (Fisher scientific Karlsruhe, Germany). The composition of

the formulations is presented Table 1.

2.3. Three-point bend test

Filament flexibility and brittleness are critical parameters for FDM-3D printing. The method used to assess filament mechanical properties was developed using specific methodologies herein referred to as Repka-Zhang test (Zhang et al., 2019). Tests were carried out using a Texture Analyzer TX-700 (Lamy Rheology, France) and a T probe with a 25 mm support gap. Samples of 6 cm length of filament were collected and placed on the sample holder. The probe moved at a speed of 10 mm/s until reaching a maximum distance of 10 mm below the sample. The test was repeated 10 times for each filament formulation. The strain/distance data were recorded and analyzed using Exponents software (Rheotex, Lamy Rheology, France) and the flexural stress (σ_f) and strain (ε_f) were calculated following equations (1) and (2) (Prasad et al., 2019).

$$\sigma_f = \frac{FL}{\pi R^3} \quad (1)$$

$$\varepsilon_f = \frac{600\delta h}{L^2} \quad (2)$$

F is the applied force (N), L the support-span (mm), R the sample radius (mm), δ the maximum deflection of the filament (mm) and h the thickness of the sample (mm). The flexural modulus was determined as the slope of the linear region of the flexural stress-strain graph between 1 and 5 % strain.

2.4. Fused deposition modelling

The model used to print the dosage forms was designed using One-shape software. The printed forms dimensions were set at 13 × 19 × 2.5 mm (width × length × heights) in order to develop an easy-to-handle form by referring to currently marketed oral dosage forms. Then, the printing parameters were selected on IdeaMaker, with no continuous outer layer (altitude shell) or continuous bottom/top layer. The grid pattern was selected for an infill presenting a density of 50 %. The Raise Pro 2 3D-printer (LeapFrog, Netherlands) and the in-built software were used for FDM. 3D-printing was performed using a $d = 0.4$ mm nozzle at a speed of 5 mm/min and a height of 0.5 mm. The lowest possible printing temperature allowing appropriate processability of the formulation was determined iteratively (data not shown). The 3D-printed forms were weighed and their dimensions were measured ($n = 10$) manually using a caliper. To reach higher drug content, printed forms height and infill density were increased to 7.5 mm and 80 %.

2.5. Physico-chemical characterization

2.5.1. Scanning electron microscopy

The surface of filaments was recorded with a scanning electron microscopy (SEM) using a Hitachi S4800 microscope operating at 2 kV. Samples were fixed to a metal pad using carbon adhesive and metallized by platinum deposition.

Table 1

Composition of the formulations (% w/w).

Formulation	PEO	PEG35K	PEG6K	VAL
F1	100	–	–	–
F2	70	30	–	–
F3	70	–	30	–
F4	67	23	–	10
F5	49	21	–	30
F6	67	–	23	10
F7	49	–	21	30

2.5.2. Thermogravimetric analysis

For thermogravimetric analysis (TGA), 5 to 10 mg of samples (powder, filament and 3D printed form cut in small pieces) were placed in a ceramic pan and then heated from 30 °C to 600 °C at a heating rate of 10 °C/min with a Perkin Elmer STA 6000 Simultaneous Thermal analyzer (Perkin Elmer, France). All experiments were carried out under a nitrogen flow of 20 ml/min. Data collection and analysis were performed using a Universal Analysis 2000 (TA instruments, Waters Corporation, New Castle, DE, USA) and percentage mass loss and/or onset temperature were calculated.

2.5.3. Differential Scanning Calorimetry

Differential Scanning Calorimetry (DSC) measurements were performed using a DSC 1 (METTLER TOLEDO, France) under a 20 ml/min nitrogen flow on powder, filament and 3D printed form cut in small pieces. Samples between 5 and 10 mg were analyzed using pierced aluminum pans, with an empty pan used as reference. A heating rate of 20 °C/min was set between -120 °C and 200 °C. Data collection and analysis were carried out using STARE software (METTLER TOLEDO, France).

2.5.4. X-ray powder diffraction

Powders were analyzed on a quartz sample holder. Powder mixtures, filaments and 3D-printed forms were placed directly onto the surface of the sample holder. XRPD analyses were performed using a Bruker D8 Advance diffractometer (Bruker, Billerica, MA, USA) and monochromatic Cu K α 1 radiation ($\lambda = 1.5406 \text{ \AA}$, 40 kV and 40 mA). The angular range of recorded data was 4–50° 2 θ , with a stepwise size of 0.02° and a speed of 0.1 s counting time per step, using a LINXEYE detector 1D.

2.6. Pharmacotechnical characterization

2.6.1. Determination of the drug loading

3D printed tablets (n = 10) were placed in 25 ml beakers and dissolved in 10 ml of ultrapure water. Samples were analyzed using HPLC on a Shimadzu system (Kyoto, Japan) equipped with an LC-20AD pump, a refractive index detector (RID-10A) and a FRC-10A fraction collector. Detector's temperature was set at 40 °C. Separation was carried out using a Shodex OHPak SB-802H polyhydroxymethacrylate column (300 mm \times 8 mm). A water mobile phase was used as eluent at 40 °C with a flow rate of 1 ml/min for 60 min. 50 μ L of sample were injected. The limit of quantification and detections were 30 μ g/ml and 10 μ g/ml respectively.

2.6.2. Disintegration test

Disintegration time was measured using a ZT 31 disintegrating apparatus, (ERWEKA, Germany) with 800 ml of distilled water at 25 °C until complete disintegration of the printed forms (n = 6) (adapted to Eu. Ph. 11.3, 2024).

2.6.3. Dissolution test

Dissolution was performed with a Dissolution tester PT-DT70 (Pharmatest, Germany) (USP apparatus II). The dissolution medium at pH 1.2 was prepared with 2 g/l of sodium chloride in 0.1 N HCl (Eu. Ph. 11.5, 2024). The dissolution medium volume was adapted to reach a concentration of VAL in the limit of quantification (30 μ g/ml). Dissolution tests in beakers were considered, but using a stirring bar would accelerate the erosion of the printed form and thus the modify the dissolution profile. Thus, the dissolution tests were performed using a USP apparatus II with 250 ml for the low VAL loaded printed forms. With the volume used, the sink conditions were respected, with a solubility/solution concentration ratio > 3 for all the samples. Thus, printed forms were placed in 250 or 900 ml, set for 50 rpm rotation speed. Samples were collected at 5, 10, 20, 30, 45, 60, 90 and 120 min and VAL was quantified (method described in part 2.6.1). Cumulative VAL

dissolved were calculated based on the nominal value of the initial formulation.

2.7. Stability study

As PEO, PEG and VAL are hygroscopic, VAL-loaded filament and printed forms (F4, F5 and F6) were stored at room temperature (20 to 25 °C) and a relative humidity (RH) of 40 % in a dry cabinet Drybox ADL-3D77, EurekaDryTech (ERM Automatisme, Carpentras, France). The temperature and humidity of the environment were monitored using a Traceable® hygrometer (Fisher scientific Karlsruhe, Germany). After 3-months of storage, 3-points bend test were performed on filaments (method described in part 2.3) and their printability was investigated. Printed forms were weighted and VAL-content was assessed as presented part 2.6.1. All the samples were analyzed using XRPD.

3. Results

3.1. Thermogravimetric analysis

The degradation onset temperature was set at 3 % (T3%). The degradation temperatures were identified at 405 °C for VAL, 352 °C for PEO and at 338 °C and 198 °C for PEG6K and PEG35K respectively (Fig. 1.a).

3.2. Differential Scanning Calorimetry

Differential Scanning Calorimetry (DSC) was used to determine phase transitions such as melting (T_m) and glass transitions (T_g) of the pure materials and the blends. T_m is observed as a peak while T_g is characterized by a slope not always clearly visible (Supplementary data Fig. S1 and S2), thus, the values of T_m (onset) and T_g are presented when they were identifiable (Table 1).

The DSC thermograms also provides information on components' interactions in the mixture, observed through the variation of the T_g and T_m. At temperature below T_g, the polymer is in a glassy state and changes to a viscous rubbery state when it reaches its T_g. The inclusion of plasticizers tends to decrease T_g by reducing polymers' chain interactions while inorganic fillers tend to increase it (Aho et al., 2015; Hess et al., 2024). T_m of a blend provides information on its homogeneity in case of single T_m or on segregation, with several T_m. In HME and FDM printing, T_m is commonly used to characterize drug's physical state throughout the process. Decrease or disappearance of drug's T_m during the process, from physical mixture to filaments or printed forms, indicates API's amorphization or dissolution in the melted polymer. Thus, T_g and T_m values were compared for physical mixtures, filaments and printed forms to assess any changes due to interactions or process's effects.

The DSC thermogram of the PEO display a T_m at 69 °C while the T_g, indicated at -67 °C by the provider, could not be determined. PEO has been reported to form crystalline complexes with barbiturates, guanidine hydrochloride and urea, as an exothermic peak between drug and polymers was observed on the physical mixture's thermograms. Without new peak on the physical mixture DSC thermograms (F4, F5, F6), our results suggest that VAL-PEO complex formation did not occur (Zhang et al., 2019). The DSC thermograms of PEG6K and PEG35K display T_m at 68 °C and 63 °C respectively and as for the PEO, the T_g were could not be determined. For VAL, the DSC thermogram exhibited an endothermic peak at 94 °C linked to water evaporation. Another peak was observed at 140 °C, which is not related to its T_g or T_m, but attributed to VAL thermal events (Chang, 1979; Petrushevski et al., 2008). As VAL has no T_m, DSC analysis in our study does not allow to conclude on its possible amorphization or dissolution in the melted polymer. Still, F4 and F5 display the same T_g at -46 °C while, for PEO-PEG6K based formulations the T_g of F6 is at -42 °C and increases to -36 °C for F7, suggesting that VAL affects the mobility of PEG6K in the amorphous part. Finally, a

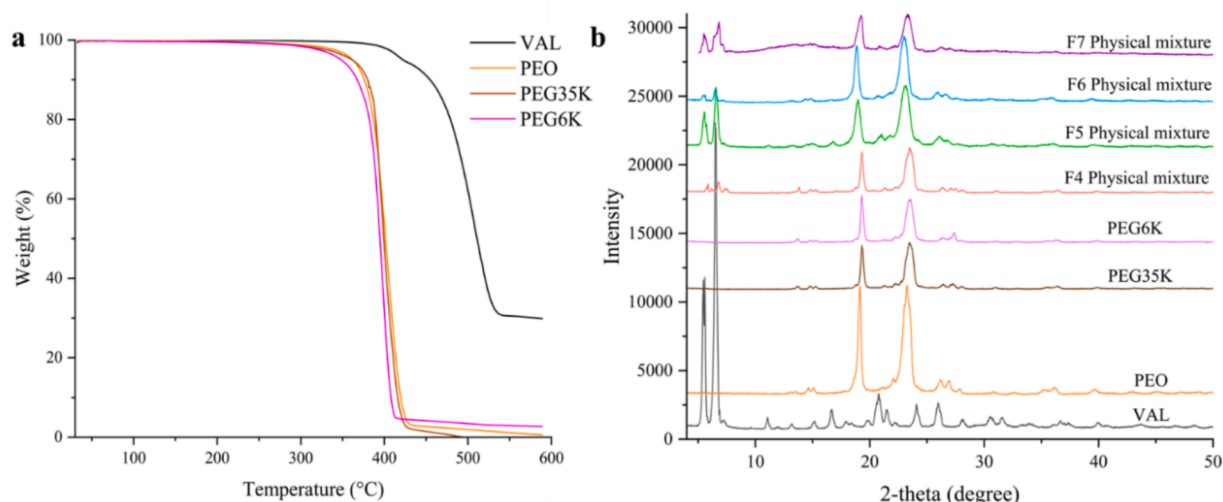


Fig. 1. a Weight loss of pure PEO, PEGs and VAL. Fig. 1.b. X-ray powder diffractograms of powder blends, PEO, PEGs and VAL.

single melting peak was observed around 52 °C was observed for all the physical mixtures (F4, F5, F6 and F7), indicating the miscibility of the components (Hess et al., 2024).

3.3. X-ray powder diffraction

X-ray powder diffraction (XRPD) analyzes were performed to investigate the physical form of VAL throughout the process (Fig. 1.b). The XRPD pattern of pure VAL exhibits its crystalline structure with two intense characteristic peaks at 6° and 7° (2 θ). PEO and both PEG35K and PEG6K display similar XRPD patterns, with Bragg peaks at 19° and 23°. The VAL and PEO/PEGs peaks are also observed for the powder mixtures F4, F5, F6 and F7 confirming the crystallinity of all the components (Teixeira et al., 2006). The intensity variations observed between powder mixture is due to the dilution effect, with less VAL in F4 and F6.

3.4. Rheological study: Flowing properties

As formulation's flowing property is a key parameter in HME and FDM, the effect of VAL loading on viscosity was determined using small amplitude oscillatory shear (SAOS) measurements at 70 °C. First, a strain sweep at an angular frequency of 1 Hz = 6.28 rad/s was performed to determine the linear viscoelastic range (LVE). The storage modulus G' , represent the elastic behavior of the material while the low modulus G'' corresponds to the viscous behavior. Over the LVE, G' and G'' usually decrease and vary with the strain amplitude. However, for suspensions nonlinear behavior may be observed with increasing G'' or decreasing G' over the LVE due to structural change at high strain amplitude. As the nonlinearity is often observed first in the elastic properties, only G' is presented here (Aho et al., 2015). Pure PEO (F1), with PEG35K (F2) and with PEG6K (F3) exhibited a slight G' decrease over 10 % indicating the LVE limit. With PEG inclusion, PEO's G'

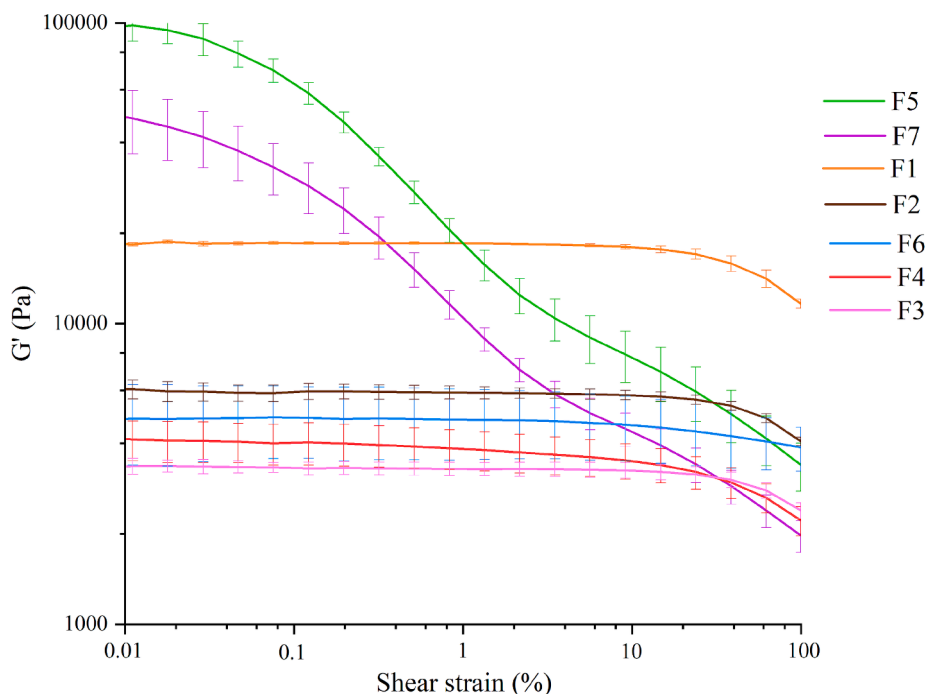


Fig. 2. Storage modulus at 70 °C and 50 rpm.

decreased from 18.3×10^3 Pa to 5×10^3 Pa with PEG35K and to 3×10^3 Pa with PEG6K, due to their plasticizing effect. Inclusion of 10 % (w/w) of VAL in PEO-PEG35K (F4) decreased G' to 4.1×10^3 Pa, indicating also a plasticizing effect). However, in PEO-PEG6K, 10 % (w/w) of VAL loading (F6) tends to increase G' to $4,8 \times 10^3$ Pa.

In general, higher solid particle content reduces the LVE range. Thus, highly concentrated suspension has a narrow or almost inexistent LVE, which is difficult for their fundamental SAOS analysis. This phenomenon is observed for formulations with 30 % (w/w) of VAL, with a sharp decrease of G' over 0.05 % for F5 and F7 (Fig. 2). These results suggest that at high VAL content, solid particles are suspended in PEO-PEG, increasing the complex viscosity.

Based on the LVE of all the formulations a strain amplitude of 0.01 % was selected for the consecutive SAOS measurements of. Then, the effect of VAL on PEO-PEGs blends was evaluated using the normalized viscosity calculated with Equation (3).

$$\eta_{norm} = \frac{\eta_{VAL-PEO}}{\eta_{PEO}} \quad (3)$$

With η_{PEO} and $\eta_{VAL-PEO}$ the absolute values of complex viscosity of pure PEO and blend of PEO and VAL.

As presented in the work of Yang et al. or Aho et al., the η_{norm} obtained at strain amplitude 0.1, 0.5, 1, 5, 10 and 100 Hz were plotted against drug content (Fig. 3).

The inclusion of 10 % (w/w) VAL in PEO-PEG35K tends to decrease the blend's viscosity acting as a plasticizer ($\eta_{norm} < 1$). At higher VAL content (30 % (w/w)) the plasticizing effect of VAL is dominated by the undissolved crystal particles, increasing the blend's viscosity as observed with the higher η_{norm} (Fig. 3.a). These result show that VAL is partially or completely dissolved in the PEO-PEG35K matrix at 10 % (w/w) while it is over its saturation concentration at 30 % (w/w) (Aho et al., 2015). For the PEO-PEG6K polymeric matrix, the η_{norm} is significantly higher than 1 with both VAL's concentration, indicating little or no VAL solubilization (Fig. 3.b).

This was also reported in the study of Aho et al. on the rheological properties of PEO with various APIs (paracetamol, ibuprofen and indomethacin). Up to 30 to 50 % (w/w) of APIs, the viscosity decreases or remains stable. For an API load exceeding its solubility in the polymeric carrier, solid particles are suspended in the melted polymeric matrix. The undissolved API acts as an inorganic filler and at high concentration, particles are believed to form networks that requires a specific stress threshold, known as yield stress to break down. This phenomenon leads to a substantial viscosity increase at low deformation rates (Aho et al., 2015). The modification of the rheological properties of the formulations can suggest VAL's percolation threshold. Several studies investigated the effect of drug loading on formulation's

properties to determine a percolation threshold (Linares et al., 2021; Mora-Castaño et al., 2022). Our study focuses on two VAL loading limiting the determination of VAL percolation threshold, still it may be interesting to investigate it in further studies with several VAL loading.

Still, the differences observed for VAL inclusion in formulations with both plasticizers suggests a better solubility of VAL in PEO-PEG35K than in PEO-PEG6K. From these results, the saturation concentration of VAL is lower than 10 % (w/w) for PEO-PEG6K, and between 10 and 30 % (w/w) of VAL for PEO-PEG35K. In a similar study on the effect of several APIs on PEO complex viscosity PEO, the drug's plasticizing effect was observed for $\eta_{norm} < 1$, due to its solubilization in the polymer. An optical microscopy study of the physical mixture, at the temperature used for the rheological study, exhibited solid particles, indicating only a partial API's dissolution. Thus, the author concluded that a decreased of η_{norm} just provides general information about drug solubilization and does not necessarily imply complete drug dissolution. Based on these results, extrusion tests were performed with all the formulations to assess the effect of VAL loading in both polymeric matrices.

3.5. Hot-melt extrusion processability

During HME process, filament's diameter was measured and adjusted to meet the specification limits of 1.75 ± 0.05 mm, required for the employed 3D printer. If needed, filament's diameter was adjusted by varying the speed of the conveyor by stretching the filament. Barrel temperature of extrusion was maintained at 70 °C and the twin-screw speed was set at 50 rpm for all the formulations. Based on the TGA results (Part 3.1) of the pure materials (VAL, PEO and PEGs) no thermal degradation is expected. As the energy required to extrude a material is directly related to its viscosity, increasing melt viscosity, will increase the torque during the extrusion (Aho et al., 2015). Thus, the torque was recorded during the extrusion to evaluate formulation's melt behavior during extrusion and compare the torque to the complex viscosity trend

Table 2

Glass transition, Tg and melting temperature, Tm from DSC analysis of pure VAL, PEO and PEGs and physical mixtures.

	Powder	Tg (°C)	Tm (°C)
Pure material	VAL	–	–
	PEO (F1)	–	69
	PEG35K	–	68
	PEG6K	–	63
Physical mixture	F4	–46	55
	F5	–46	50
	F6	–42	52
	F7	–36	–54

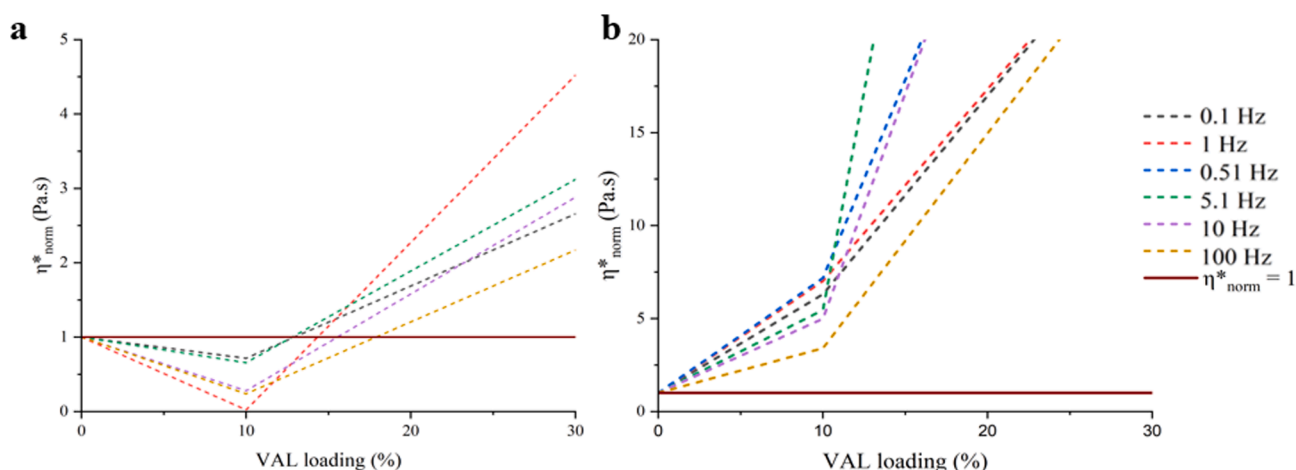


Fig. 3. Normalized viscosity as a function of VAL loading. Fig. 3.a PEO-PEG35K. Fig. 3.b PEO-PEG6K.

(Table 2).

A torque decrease is observed from 0.46 N.m for pure PEO (F1) to 0.34 N.m (F2) and 0.31 N.m (F3) due to PEGs' plasticizing effect (Table 2). For F4, a slight decrease to 0.31 is observed while it increased to 0.40 N.m for F5, which may be attributed to the high amount of VAL (30 % (w/w)), which is consistent with the viscosity increase observed in part 3.4. Filaments F1, F2, F3 and F4 were successfully extruded with a controlled diameter matching the requirement of the 3D printer of 1.75 ± 0.05 mm. While filaments with 30 % (w/w) of VAL (F5) displayed higher diameter's deviation. Still, filament F5 matched the requirement (1.73 ± 0.02 mm). Surprisingly, a torque decrease is observed for both PEO-PEG6K based formulations, from 0.31 N.m to 0.22 N.m (F6) and 0.24 N.m (F7), which contradict the rheological measurement. The significant torque decrease can be due to PEG6K acting as a lubricant during extrusion. Xie et al. reported this property during the extrusion of highly viscous polymers (polyethylene/polypropylene). PEG6K tend to migrate onto the extruder's walls to reduce the viscous dissipation and the free energy of the system. The author attributed this phenomenon to the higher surface tension of PEG6K and to its small size leading to an external and internal lubricant effect. In fact, SEM and infra-red spectroscopy analysis of the filament showed PEG6K located on the surface but also inside the sample, due to its plasticizing effect (Xie et al., 2010). Thus, in our study, it can be suggested that inclusion of 30 % (w/w) of VAL in PEO-PEG6K, increased the viscosity of the formulation F7, leading to PEG6K's migration acting as a lubricant which result to a torque decrease. This phenomenon is not observed with PEG35K and, to our knowledge, has not been reported in literature, but it can be supposed that PEG35K's polymer chains, longer than PEG6K's hindered its movement. Despite the torque decrease observed for formulation F6, a filament with controlled diameter could be prepared while it was not possible for F7 due to significant diameter's deviation.

These results highlight the importance of the plasticizer's molecular weight regarding the drug amount that can be loaded to obtain a suitable filament for FDM printing. As the fluctuating diameter of the filament is not suitable for FDM printing to develop precisely controlled dosage forms, the F7 filament was not retained for 3D printing.

Filaments F1, F2 and F3 were visually observed to be flexible and transparent (Fig. 4a). Overall, VAL loaded filaments resulted in white filaments. The visually observed increasing opacity of filaments with increasing VAL loading could indicate that the drug was not melted or dissolved in the polymer matrix remaining in a crystalline state, which need to be confirmed by XRPD (presented part 3.3) (Tidau et al., 2019).

3.6. Filament's characterization

3.6.1. Quantification of VAL: filament's homogeneity

First, filament's VAL content was quantified, in order to verify its homogeneity, otherwise the filament would not be adapted to prepare FDM printed forms (Supplementary data Table S1). Filaments F4 and F6 displayed 10.0 ± 1 and 9.85 ± 1 % (w/w) of VAL, close to the expected theoretic content of 10 % (w/w). For filament's F5, the drug content is also close to the target of 30 % (w/w) with 29.1 ± 2 % (w/w). However, for filament F7 the VAL content of 27.0 ± 4 % (w/w), is lower than 30 % (w/w) and shows a higher deviation than the others filaments. This can be attributed to filament's diameter observed during HME (part 3.5) leading to large dose variations. Thus, filament F7 is unsuitable for FDM printing, still it will be characterized to be compared with the others formulations.

3.6.2. SEM: filament's surface morphology

Microstructural investigation of filaments via SEM revealed visible crystal particles on the surface of VAL loaded filaments (Fig. 5). As these particles are not observed on filament F2 and F3 used as references, without API, these crystals are identified as VAL. The surface of loaded filaments F4, F5, F6 and F7 is rough compared to filaments F2 and F3

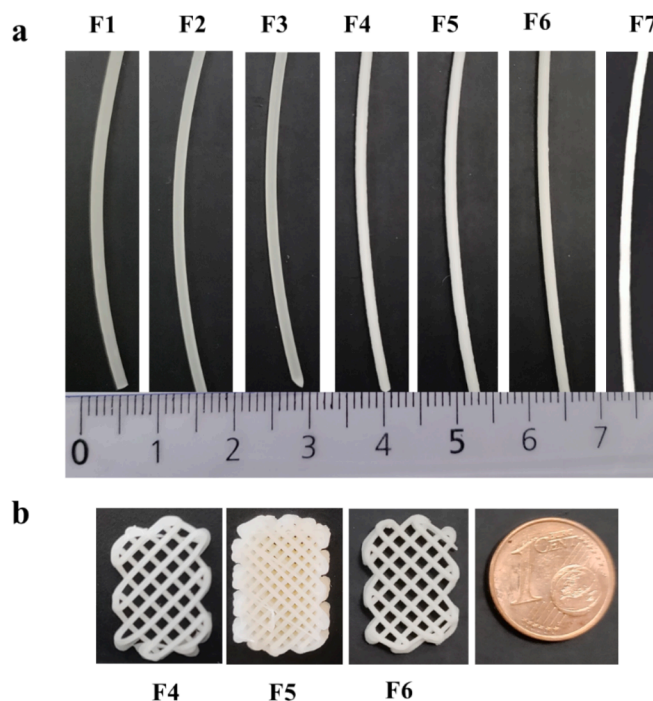


Fig. 4. A. Picture showing the filaments produced by HME at 70 °C and 50 rpm (scale in cm). b. Picture showing the printed forms from formulations F4, F5 and F6.

and asperities seem to increase with higher VAL content at 30 % for filament F5 and F7 (Fig. 5.d and 5.f). This has also been reported with HPMC extruded with prednisolone which is not completely melted and mixed with the polymer over 20 % (w/w) (Larsen et al., 2024). Similarly, this phenomenon has been reported for non-melting fillers such as tri-calcium phosphate with Eudragit® EPO, leading to an increase in filament's roughness (Sadia et al., 2016). Moreover, particle-related effect of the printing process has been reported with API crystal which may increase the viscosity of the melted blend and induce temporary blockage when the diameter is reduced within the hot nozzle (Tidau et al., 2019).

3.6.3. XRPD

Filaments were characterized using XRPD and no significant differences were observed between their surface and their cross section. VAL crystallinity is also confirmed by the XRPD patterns as a characteristic peak is observed in the loaded filaments (F4, F5, F6 and F7) (Fig. 6). Filament with 10 % (w/w) of VAL (F4 and F6) display the same VAL peak as physical mixture, while for filaments F5 and F7 (30 % (w/w) VAL), the crystalline peaks of VAL are broader suggesting a partial API's dissolution within the polymeric matrix during the extrusion (dos Santos et al., 2022; Kimura et al., 2019). Moreover, a decrease in PEO and PEGs peaks' intensity is observed, for all the filaments suggesting an amorphization of the polymeric matrix during extrusion.

3.6.4. Thermal analysis

The TGA analysis show a mass decrease between 30 and 100 °C due to water evaporation, estimated at 2 and 3 % (w/w) for F35-10 and F6-10, and up to 6 and 7 % (w/w) for F5 and F7 (Supplementary data Fig. S3). These analyses confirm the hygroscopic property of VAL, promoting water absorption, which can modify filament's thermal and mechanical properties. Thus, the broadening of VAL's diffractions peaks observed in XRPD may therefore be related to VAL solubilization in the polymeric matrix and in residual water.

The comparison of sample's T_g and T_m, before (physical mixture) and after extrusion (filament) display a trend toward lower

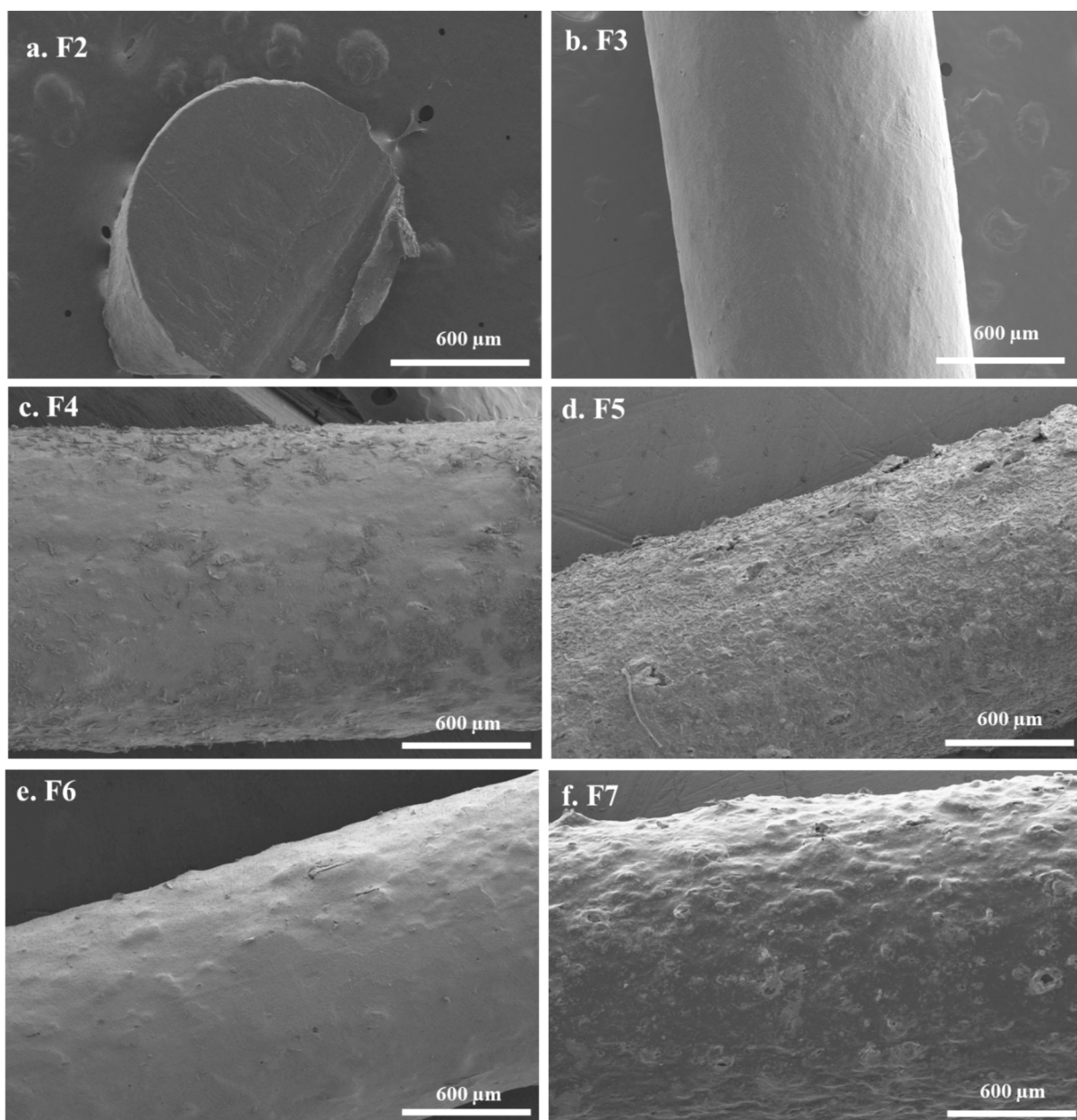


Fig. 5. SEM pictures of filaments.

characteristics temperature (Table 3) (Supplementary data Fig. S4 and S5). The T_g represents the amorphous part of the polymer while T_m is related to the crystalline part (Aho et al., 2016). A T_g decrease is observed for F4 ($-12\text{ }^\circ\text{C}$) and F6 ($-4\text{ }^\circ\text{C}$) while a $3\text{ }^\circ\text{C}$ T_g increase is observed for F7 and no significant variation for F5. These results suggest that during HME, for a same drug loading (10 % (w/w)), VAL inserts more easily between PEO-PEG35K chains than between PEO-PEG6K, leading to a better plasticizing effect, which confirm the rheological study. No significant variation in T_m was observed for F4 and F7 while an increase of $8\text{ }^\circ\text{C}$ was observed for F5 and F6, suggesting an effect of VAL on the crystalline part of the polymer during the transition from powder to filament.

Then, the T_g and T_m of filaments are compared as a function of VAL content. No significant T_g differences are observed between PEO-PEG35K based-filament (F2) ($-61\text{ }^\circ\text{C}$) and F4 with 10 % (w/w) of VAL (F4) ($-58\text{ }^\circ\text{C}$), while with 30 % w/w of VAL (F5), the T_g is $16\text{ }^\circ\text{C}$ higher ($-45\text{ }^\circ\text{C}$). These observations tend to confirm that VAL is partially dissolved in PEO-PEG35K at 10 % (w/w) while it reaches a

saturation concentration and remain undissolved at 30 % (w/w), as observed in the rheological study (part 3.4). This phenomenon has been reported for others PAs in PEO, which above the saturation concentration, are no longer dissolved in the polymer and exists in the form of crystalline or amorphous particles. This undissolved API can act as solid filler which may affect the blend's thermal properties. A study on PLA with inorganic particles as filler, shown a T_g increase with the filler content. According to the authors, this can be attributed to the agglomeration of the inorganic particles reducing the mobility of the polymeric chains, requiring more energy to move. In our study, it can be suggested that at 30 % (w/w) undissolved VAL acts as inorganic particles limiting PEO and PEG35K movement and increasing T_g . Thus, even with residual water in the filament with plasticizing properties, VAL inclusion decreases polymer's mobility and increase T_g (Liu et al., 2014).

For PEO-PEG6K, a T_g shift to higher temperature is observed with increasing VAL loading, from $-55\text{ }^\circ\text{C}$ (F3) to $-46\text{ }^\circ\text{C}$ with 10 % (w/w) of VAL (F6) and -37 with 30 % (w/w) (F7). These results align with the

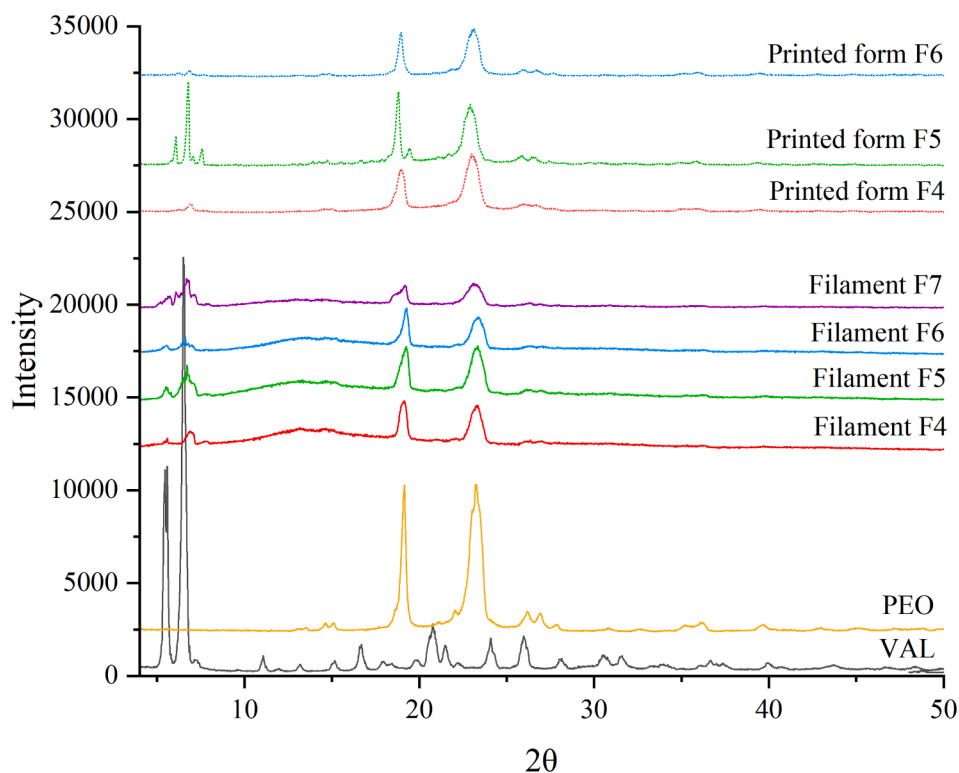


Fig. 6. X-ray powder diffractograms of VAL, PEO, filaments F4, F5, F6 and F7 (solid line) and printed forms F4, F5 and F6 (dash dot).

Table 3

Viscosity, torque and mean filament's diameter for the tested formulations.

Formulation	Torque (N.m)	Filament diameter (mm)
F1	0.46 ± 0.02	1.74 ± 0.04
F2	0.34 ± 0.02	1.75 ± 0.02
F3	0.31 ± 0.02	1.76 ± 0.04
F4	0.31 ± 0.02	1.76 ± 0.03
F5	0.40 ± 0.01	1.73 ± 0.02
F6	0.22 ± 0.01	1.74 ± 0.01
F7	0.24 ± 0.01	–

rheological study, indicating undissolved VAL in PEO-PEG6K, even at low drug loading (F6).

3.6.5. 3-points bend test

During FDM 3D printing, the filament is exposed to stress induced by the continuous driving of the feeding gears, as well as the pressure exerted to pass through the nozzle. Thus, the filament is exposed to tensile compression stresses. Therefore, a filament would be printable if it displays mechanical properties, to avoid filament bending and breakage during this process. To study the mechanical properties of the filaments, 3-points bend tests were performed to compare filaments knowing that the greater the breaking distance is better filament's flexibility (Zhang et al., 2019).

The flexural modulus (E_f) derived from the strain/distance curve was considered as an indicator of filament processability in FDM (Fig. 7). Filaments of pure PEO (F1), PEO-PEG35K (F2) and PEO-PEG6K (F3) displayed a E_f 16, 17 and 14.5 MPa respectively. The lower E_f with PEG6K confirms its higher plasticizing effect than PEG35K. With VAL inclusion in PEO-PEG35K, filament's E_f decreases of 24 % for F4 (13 MPa) and 18 % for F5 (14 MPa). While for PEO-PEG6K filament's E_f decreases of 31 % (10 MPa) for both drug loading (F6 and F7).

The effect of drug loading has been investigated for paracetamol in HPMC. Formulations without API are mainly composed of long polymer chains interacting together, inclusion of paracetamol lead to a

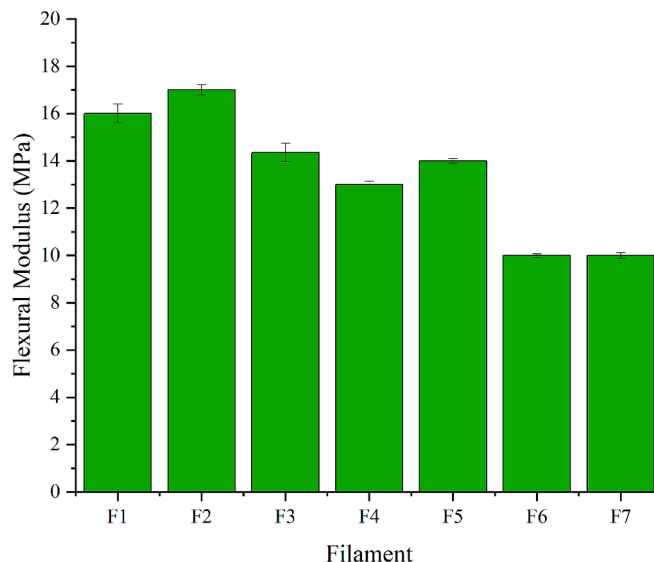


Fig. 7. Flexural modulus (E_f) of filaments F1 to F7.

plasticizing effect as observed with E_f decrease from 4.4 MPa to 0.2 MPa. However, over the paracetamol's saturation limit (50 % (w/w)), filament's E_f increased to 3.8 MPa (Prasad et al., 2019). Surprisingly in our case, no significant E_f variation are observed with increasing VAL loading. However, as observed in TGA analysis, filament's water content increases with VAL, and water is known to act as plasticizer, increasing filament's flexibility, thus a E_f decrease is expected. At the same time, XRPD and SEM analysis shown undissolved crystalline VAL particles in all the filaments (F4, F5, F6 and F7), which may act as filler and increase E_f . Thus, it can be suggested that there is a competition effect between the water's plasticizing effect, which tends to reduce E_f and VAL which tends to increase it, resulting in an E_f independent of VAL loading.

3.7. Fused deposition modeling 3D printing

The printing temperature is often higher than the HME processing temperature due to the absence of screw inducing shear stress to help soften the filament. The recommended nozzle temperature needed for successful printing is approximately 10 to 40 °C higher than the HME processing temperature. The printing temperature are presented in Table 4 (Samaro et al., 2020).

All the filament were suitable for FDM printing, this suggest that filament with a Ef of 10 MPa are suitable for FDM printing. For each filament, the printing temperature was determined iteratively, by increasing the nozzle temperature in 5 °C increment until 10 consecutive prints could be repeated without flow inconsistencies (data not shown). Filament of pure PEO (F1) was printed at 120 °C while with PEG35K (F2) and PEG6K (F3), the printing was successfully achieved at 100 °C (Table 4). PEGs have been reported to plasticize polymers resulting in a good melting of the filaments in the nozzle with a consistent flow of the material at lower temperature than pure polymer (Hess et al., 2024; Yu et al., 2015). However, for filaments loaded with 10 % w/w of VAL (F4 and F6) the flow was inconsistent at 100 °C. The temperature has to be raised to 110 °C to ensure a constant flow for both filaments. Finally, to ensure an appropriate flow behavior with filament F5, the printing temperature was increased up to 140 °C to avoid nozzle clogging and achieve reproducible printing. Increasing VAL content, led to filament whitening due to undissolved particles, as observed in Part 3.6 which may affect the flow behavior of the melted formulations. Moreover, the rheological study shows that inclusion of 30 % (w/w) of VAL increases the complex viscosity (Part 3.4). Thus, a printing temperature was required to decrease polymer's viscosity and improve their flow through the nozzle carrying VAL particles. The same observations were reported for a 3D printed theophylline HPMC-based filament, requiring higher printing temperatures with increasing theophylline loading (Tidau et al., 2019).

Still, all formulations with VAL were successfully printed as shown in Fig. 4b. A grid pattern was selected for all the printed forms to increase the surface-to-volume ratio and thus improve the disintegration time as demonstrated in previous studies (Goyanes et al., 2015; Yu et al., 2020). Two printed forms were design to develop to achieve both low and high API's dose to cover a wide range of patients. Low drug loaded printed forms of 2.5 mm height and an infill density of 50 % were prepared with filaments F4 and F6 (10 % (w/w) VAL). For the high drug loaded form the infill density of 80 % and the height were increased to 80 % and 7.5 mm and prepared with filament F5.

3.8. Characterization of the printed forms

TGA of printed forms with 10 % (w/w) of VAL (F4 and F6) display a mass loss of 2.5 % (w/w) between 30 and 100 °C (Supplementary data Fig. S6). Thus, the water content in filaments and printed forms is similar. However, for printed form F5 (with 30 % (w/w) of VAL, a decrease in water content is observed from 6 to 4 % (w/w) after printing. The differences observed between formulation with 10 % and 30 % (w/w) of VAL can be attributed to the higher printing temperature for F5 (140 °C) compared to 110 °C for F4 and F6.

After FDM printing, the XRPD patterns of the 3 printed forms do not

Table 4
Glass transition (Tg) and melting temperatures from DSC analysis of filaments.

Formulation	Tg (°C)	Tm (°C)
F1	-60	57
F2	-61	57
F3	-55	57
F4	-58	56
F5	-45	58
F6	-46	57
F7	-37	55

display the amorphization peak observed in filament (Fig. 6). Moreover, the diffractogram of printed forms F5 displays an intense et sharper VAL's peak, indicating its recrystallization during 3D printing, while it decreased for formulations loaded at 10 % w/w (F4 and F6). For these forms, the Bragg peak at 6° (20) is no longer visible while the peak at 7° is still observed with a low intensity. This suggest a rearrangement of VAL through interactions with the polymer matrix leading to its partial amorphization during the printing process of F4 and F6, which is reported in literature for other drugs (Hoffmann et al., 2023). The differences observed between F4, F6 and F5 can be due to the higher printing temperature for filament F5, leading to water evaporation, as observed in TGA, which may promote VAL recrystallization (140 °C).

The comparison of filament and printed forms' Tg and Tm display a shift to higher temperature after FDM printing (Table 5). The Tg increase can be attributed to the water loss observed in TGA, due to its evaporation during FDM printing. And the Tm increase can be due to higher crystallinity of PEO/PEGs in F4 and F6, and also VAL for F5, as observed on printed forms XRPD diffractograms (Fig. 6) (Supplementary data Fig. S7 and S8).

Then Tg and Tm of printed forms are compared to assess the effect of VAL content in each matrix. For PEO-PEG35K, a Tg increase of 3 °C with 10 % (w/w) of VAL (F4) and 8 °C with 30 % (w/w) of VAL (F5). While, for PEO-PEG6K, the Tg of F3 increases from -49 °C to -41 °C with 10 % (w/w) of VAL. As observed for filament (part 3.5), the higher Tg with VAL can be attributed to water evaporation promoting VAL recrystallization, increasing the amount of solid VAL particles limiting polymers mobility. The Tg increase is therefore attributed to a coupled effect of water loss, solubilizing VAL and plasticizing the filament.

3.8.1. Characterization of the printed forms: weight, size and drug content

The VAL-loaded 3D-printed forms have a size and shape in agreement with the predefined dimensions and no significant variations are observed (Table 6). According to the Eur. Ph. criteria, the variation in tablet mass is set at 7.5 % and the tolerated drug content's deviation is set at 15 % (Eu. Ph. 11.5, 2024). Thus, all the formulations meet the Eur. Ph. criteria. This demonstrates that there is no segregation or inhomogeneity induced by each step of the preparation process.

Printed forms F4 and F6 meet Eur. Ph. criteria with a mass deviation of 6.0 % or less. The drug content deviation for F4 is 2.0 % and 7.1 % for F6, indicating a better homogeneity for F4, still both formulations reach the specifications (< 15 %) Eur. Ph. Criteria. The average VAL content, in both printed forms, corresponds to the needs of a 1-month child with 20 mg per form. Formulation F5 was printed with a higher height and infill density to meet the needs of older patients. The average mass of printed form F5 (841 mg) meets the Eur. Ph. criteria with a mass deviation and a VAL content deviation of 4.8 %. The average VAL load, 247 mg, is convenient to treat patients up to 16.2 kg, (4-years-old child). Thus, VAL content deviation inter-samples in all the printed forms, is low, providing good dose reproducibility. As a result, these printed forms cover the needs of patients aged from 1-month to 4 years, with a wide range of VAL dosages (18 to 247 mg).

3.9. Disintegration test

As the target population is younger children, the printed forms are

Table 5
Printing temperatures of the formulations under study.

Formulation	Printing temperature (°C)
F1	120
F2	100
F3	100
F4	110
F5	140
F6	110
F7	-

Table 6

Glass transition and melting temperatures from the DSC analysis of the printed forms.

Formulation	Tg (°C)	Tm (°C)
F1	-49	58
F2	-50	58
F3	-49	61
F4	-47	58
F5	-42	57
F6	-41	55

designed to disintegrate quickly in water before being administrated via a syringe or baby bottle. During the test, progressive erosion of the printed forms was observed. The printed form was designed with a grid pattern without a shell to enhance water contact. The grid was printed by successive deposition of melted blend through lines joined by a crossing point (Fig. S9). As a result, the thinner areas (lines) erode more quickly than the crossing points, leading to particles of less than 2 mm suspended in water after 3 to 5 min for small printed forms and after 10 min for the biggest (F5). As mini-tablets of 2 mm diameter are well accepted among children, the printed forms can be administrated as a suspension (Quodbach et al., 2022). Similar results were obtained by Roulon et al., who carried out a disintegration test with 5 ml of water in syringe and resulted on disintegration time of 3 to 5 min, with increasing size of the printed form (100 to 300 mg). As observed in our study, the main disintegration mechanism was erosion due to the high quantity of PEO in the formulation (Roulon et al., 2021).

Printed forms at 50 % of infill density and 2.5 mm height were completed dispersed after 6 to 7 min and after 15 min for the printed form at 80 % infill density and 7.5 mm height. Thus, the printed forms does not reach the Eur. Ph. (2.9.1) of 3 min for dispersible tablet (Table 7) (Eu. Ph. 11.5, 2024). This has previously been reported as a limitation in the use of FDM printed forms due to the low porosity (Đuranović et al., 2021). Still, it may be possible to prepare the printed forms 6 to 15 min before administration. Table 8

3.10. Dissolution test

The dissolution results of 3D-printed forms F4, F5 and F6 in acidic medium are presented Fig. 10. Due to the low drug loading (18 mg) of the F4 and F6 printed forms (10 % (w/w) of VAL), dissolution tests were performed using 250 ml of acidic medium (pH 1.2) to reach VAL concentration above the limit of quantification (30 µg/ml) (Fig. 8.a). Due to higher drug loading of printed forms F5, the dissolution tests were performed with 900 mL according to the Eur. Ph. (Fig. 8.b) (Eu. Ph. 11.5, 2024).

The three formulations showed an immediate release with at least 80 % of VAL dissolved in than 45 min. VAL is reported as freely soluble in 0.1 N HCl (1.25 g/mL at 20 °C) (Phaechamud et al., 2010). The fast VAL release can be due to the interaction of the ether oxygen atom of PEO with the hydrogen ions in the acidic media. The resulting hydrogen bonds would induce electrostatic repulsion between the polymer chains, increasing solubility and dissolution rate of PEO, and thus, drug release (Bailey and Callard, 1959). Printed forms loaded with 10 % w/w of VAL reach 80 % of cumulative drug dissolved in 20 min (F6) and 25 min (F4). The effect of PEO and PEGs molecular weights on the dissolution rate

Table 7

Printed forms F4, F5 and F6 characteristics: infill density, average weight, size and VAL content.

Formulation	Weight (mg)	Length (mm)	Wide (mm)	Height (mm)	VAL content (mg)	
					Theoretic*	Measured
F4	182 ± 11	16.7 ± 0.4	10.5 ± 0.6	2.5 ± 0.2	18.2 ± 1.1	18.0 ± 1.7
F5	841 ± 41	16.9 ± 0.6	11.1 ± 0.9	7.7 ± 0.4	252.3 ± 12.3	247.0 ± 12
F6	185 ± 11	16.5 ± 0.3	10.4 ± 0.6	2.6 ± 0.3	18.5 ± 1.1	18.1 ± 1.1

*Derived from measured tablet weights and average VAL content in the formulations including standard deviation.

Table 8

Disintegration time of printed forms F4, F5 and F6.

Formulation	Infill density (%)	Height (mm)	Disintegration time (min)
F4	50	2.5	<7
F5	80	7.5	<15
F6	50	2.5	<7

has been widely reported (Cantin, 2016). Short polymer chains hydrate and dissolve faster than longer chains, improving the hydration of the polymer matrix. The viscosity of the hydrated layer is also decreased due to PEGs, which facilitates VAL diffusion. As a result, the dissolution rate of printed form with PEG6K (F6) is faster than that with PEG35K (F4) due to its lower molecular weight. Finally, F5 printed forms reached 80 % of dissolved VAL in 20 min. This result cannot be directly compared to F4 and F6 as the printed forms' dimensions and the volume used for the dissolution test are not the same. Nevertheless, 80 % of the drug is released in less than 45 min, which is considered as an immediate release based on the European Medicine Agency (EMA, 2016). A similar drug release profile was observed in the work of Isreb et al. who developed PEO/PEG6K-theophylline forms and achieved 80 % drug release within 20 min in an acidic media (pH 1.2) (Isreb et al., 2019).

3.11. Stability study

For the stability test, 3 m of freshly extruded filaments were wound into a spool and stored for 3-months at room temperature and 40 % of relative humidity (RH). The filament TGA after storage indicates a mass loss of 4 % for filament F4 and F6 (with 10 % (w/w) of VAL). The comparison with freshly extruded filaments indicates a 2 % water absorption during storage. This phenomenon is also observed for filament F5, with a water content increase from 6 % (before storage) to 8 % (after 3 months) (Fig. S10).

These results indicate water sorption during the storage due to the hygroscopic properties of PEO, PEGs and VAL. This aligns with the XRPD pattern, indicating a decrease of the intensity of PEO and PEGs' diffraction peaks due to a partial solubilization of the polymers in the absorbed water. The XRPD pattern also show that crystalline VAL particles remain after 3 months (Fig. S11).

Filaments F4 and F6 were printable after storage (Fig. S12) and the resulting printed form, referred as Pa (Printed after storage) meet the Eur. Pharm. Criteria of mass uniformity and drug uniformity (Table S2). However, filament F5 broke during storage, which may be attributed to the non-melted VAL particles at a concentration that exceeds VAL solubility's threshold. Due to filament's F5 breakage, only two forms could be printed, thus mass and drug loading uniformity could not be checked (Fig. S12).

As observed for filaments, the TGA of printed forms stored during 3-months, referred as Pb (printed before storage) indicate water sorption during storage. This increase in water content may have an influence on the component's physical state, on the mass of the printed forms and VAL dissolution profile. The XRPD patterns of the printed forms (Pb) and (Pa) show the PEO and PEGs peaks (Fig. S14). As observed with freshly printed forms, the peak of VAL at 6° is not visible while the peak at 7° (2θ) is observed in all the printed forms, with a low intensity for printed forms F4 and F6 and a high intensity for F5. As observed for freshly

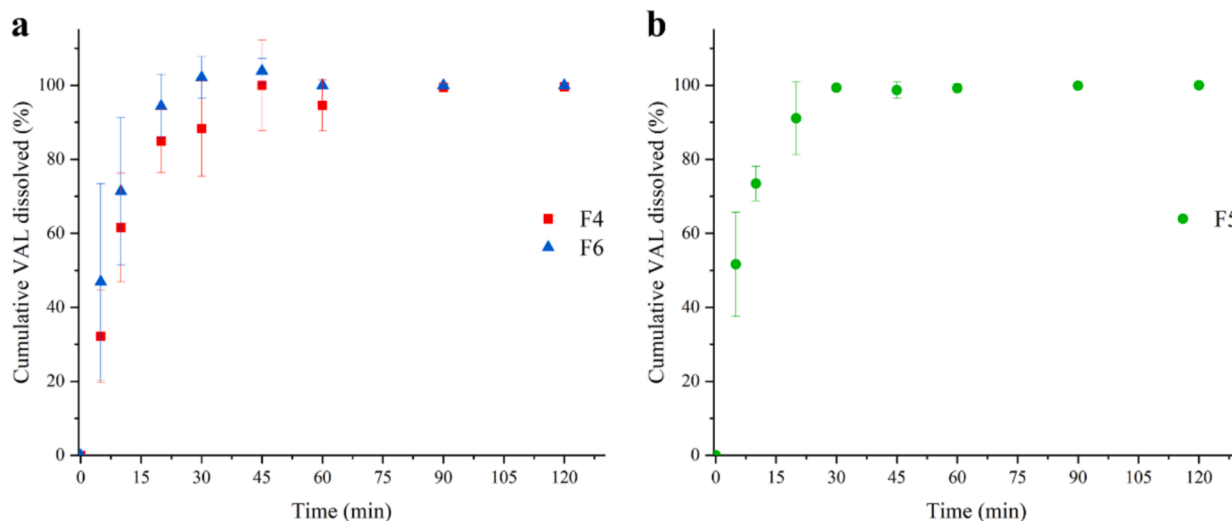


Fig. 8. Dissolution profiles of printed forms in acidic medium (pH 1.2) (n = 6). a Printed forms F4 and F6. b. Printed form F5.

printed forms, the higher printing temperature for F5 (140 °C) promotes VAL recrystallization during FDM printing. Thus, no significant variation of VAL physical state is observed in Pa and Pb in the 3 formulations.

For the three formulations, printed forms Pb and Pa were weighted, VAL-content was quantified and disintegration tests were performed. The comparison of freshly, Pa and Pb printed forms' chromatograms do not indicate VAL degradation or impurities in the stored samples (Fig. S15). The comparison of the average mass of freshly printed form (day 0) and Pa and Pb show a mass increase due to water absorption during storage, with an increase of: 4 % (Pb) and 2 % (Pa) for F4, 3 % for F5 Pb, 2 % for F6 Pa and up to 5 % for F6 Pb (Table S2). Still, despite these variations, the mass deviation reaches the Eur. Ph. criteria (< 7,5 %) for the 3 formulations. Regarding the average VAL content's variations, the highest deviation of 6,4 % (F5 Pb) remains below the 15 % set by the Eur. Ph. Finally, the disintegration of the printed form into water-suspended particles was achieved in 5 min for F4 and F6 Pa and Pb and in 10 min for F5 Pa. The disintegration is completed after 7 (F4 and F6) and 14 min (F5), thus, the storage did not affect the printed forms disintegration. Finally, dissolution tests were performed in acidic media with printed forms Pa and Pb.

No significant differences were observed for printed forms F4 Pa and Pb, with 80 % of VAL dissolved in 20 min (Fig. S16.a). The high variations are due to air bubble within the HPLC column at retention time close to VAL's, but this phenomenon also occasionally observed for the others samples, seems to be related to the purging of the column. Still the trend observed indicates an immediate release VAL reaching over 80 % release in 45 min or less. For F6 a faster VAL release is observed for printed forms Pb than PA, reaching 80 % in 15 and 20 min respectively (Fig. S16.b). This may be related to water absorption during the storage of printed forms Pb (5 %) enhancing solubilization. Finally, F5 Pb display a similar release profile to freshly printed forms with 80 % of VAL in 20 min, despite the water absorption (Fig. S16.c). Thus, the printed forms reach the EMA criteria of rapid release after 3-months storage.

4. Discussion

This study focused on the combined effect of PEG's molecular weight, as plasticizer, and VAL loading on formulation's processability. From the extrusion test, the lubricant effect of PEG6K, leading to an over plasticization of formulation F7 and resulting in poor flowing properties was observed. Thus, it was shown that only PEG35K was suitable to prepare high VAL-loaded filament (30 % (w/w)) compatible with FDM printing (1.75 ± 0.05 mm).

Filament's whitening observed for formulations F4, F5, F6 and F7, suggest VAL particles non mixed with PEO-PEG as observed in previous studies with theophylline-PEO, theophylline-HPMC or paracetamol-HPMC (Prasad et al., 2019; Tidau et al., 2019). This is confirmed with increasing filaments' roughness observed on SEM pictures which was also reported with inclusion of non-melting filler, such as tri-calcium phosphate in Eudragit® EPO, affecting filament's external appearance due to a lack of integrity (Sadia et al., 2016). Moreover, XRPD diffractograms indicate crystalline VAL particles non mixed with PEO-PEG for filaments and printed form. From these analyses no significant difference influence of the PEO-PEG35K and PEO-PEG6K polymeric matrix on VAL incorporation are observed.

However, the rheological study indicates the plasticizing effect of VAL at 10 % (w/w), decreasing the complex viscosity, though its partial dissolution in PEO-PEG35K (F4). With increasing VAL loading to 30 % (w/w) (F5), the plasticizing effect is dominated by undissolved VAL leading to suspension type VAL-loaded formulations, as observed in previous studies. While no VAL-plasticizing effect is observed with PEO-PEG6K. Aho et al, demonstrate that the drug-polymer processability depends on drug, for instance, the maximum plasticizing effect of PEO was achieved with 50 % (w/w) ibuprofen and 30 % (w/w) paracetamol. While our study shows that VAL's plasticizing effect is highly dependent on PEG's molecular weight. To investigate this further, it could be interesting to compare formulations with VAL-loading ranging from 5 to 70 % (w/w). Moreover, the comparison of filaments and printed forms' Tg with and without VAL shows PEG's influence, with a lower Tg increase with VAL inclusion in PEO-PEG35K than PEO-PEG6K. This suggest that for the same drug-loading, VAL is better incorporated into the polymeric matrix with PEG35K than PEG6K. However, it is not possible to quantify this difference, as there are not significant differences between the XRPD patterns of filament F4 and F6. Further analysis would be required to compare VAL solubility in melted blends, as has been done for others formulations using Raman spectroscopy or hot-stage microscopy (Cantin, 2016; de Assis et al., 2022; Roulon et al., 2021; Verreck et al., 2005).

The modification of the rheological and thermal properties indicates VAL solubility's limit closely related to PEG's molecular weight, suggesting a percolation threshold. Several studies have explored these phenomena using percolation theory to determine the drug's percolation threshold (Linares et al., 2021; Mora-Castaño et al., 2022). In our study, only two VAL-loading were investigated, which is limiting to determine its percolation threshold, still it could be interesting to investigate it in further study.

5. Conclusion

In this study, dispersible forms were successfully developed to provide 3D-printed personalized forms achieving a wide VAL dosage range (18 to 247 mg), suitable for patients aged 1 month (medicated with 10 mg/kg/d divided in two doses) to 4 years (medicated with 30 mg/kg/d divided in two doses). HME coupled with FDM was used to develop formulations with PEO as a water-soluble polymer carrier and two plasticizers (PEG35K and PEG6K). Formulations loaded with 10 % (w/w) of VAL were successfully extruded and printed with both plasticizers (F4 and F6), while only formulation with PEG35K was suitable to develop forms with higher VAL content (30 % (w/w)) (F5). Rheological, DSC and XRPD analyses indicate that VAL solubility's limit is higher in PEO-PEG35K than in PEO-PEG6K (less than 10 % (w/w) of VAL). These results proved that VAL solubility's in the polymer blend depends on the plasticizer molecular weight. Still, this did not affect printed forms' average mass and VAL content, reaching the targeted dosage of 18 to 247 mg. As neonates and children of few months old cannot swallow tablets, the dosage form needs to be administrated in liquid form. The grid pattern of the printed form enhanced water-contact during disintegration test, resulting in particles of less than 2 mm suspended in water after 3 to 15 min, which could be directly administrated to patients. The dissolution study showed that all printed forms achieved a rapid release, with 80 % of VAL dissolved in less than 45 min, as observed in previous a study (Isreb et al., 2019). Finally, filaments and printed forms F4 and F6 stored at room temperature and a RH of 40 % remained stable for over 3-months, with a stable average weight, drug content and dissolution profile. Filament F5 was not suitable for the stability study due to breakage during storage, which can be due to the high VAL loading. Overall, this study demonstrates the suitability of HME coupled with FDM to develop a dispersible form for the pediatric population with a high dose flexibility.

CRedit authorship contribution statement

M. Monteil: Writing – original draft, Methodology, Investigation. **N. M. Sanchez-Ballester:** Writing – review & editing, Conceptualization. **A. Aubert:** Methodology. **O. Gimello:** Investigation. **S. Begu:** Writing – review & editing, Validation, Supervision. **I. Soulaïrol:** Writing – review & editing, Validation, Supervision.

Declaration of competing interest

The authors declare that they have no known competing financial interests or personal relationships that could have appeared to influence the work reported in this paper.

Acknowledgement

The authors want to thank the university of Montpellier for the extruder's funding. The authors also want to thank Adrien Aubert for the 3D printing, Bertrand Rebiere for the SEM analysis at the European Institute of Membranes, Amine Geneste for the DSC analysis, Thomas Cacciaguera and Jeremy Rodriguez for the XRPD measurements at the Institute Charles Gerhardt Montpellier. They also would like to thank, Ms. Maillard for the training on the texturometer at the Nîmes CHU.

Appendix A. Supplementary material

Supplementary data to this article can be found online at <https://doi.org/10.1016/j.ijpharm.2025.125345>.

Data availability

Data will be made available on request.

References

- Aaberg, K.M., Gunnes, N., Bakken, I.J., Lund Soraas, C., Berntsen, A., Magnus, P., Lossius, M.I., Stoltenberg, C., Chin, R., Surén, P., 2017. Incidence and prevalence of childhood epilepsy: a nationwide cohort study. *Pediatrics* 139, e20163908.
- Aho, J., Boetker, J.P., Baldursdottir, S., Rantanen, J., 2015. Rheology as a tool for evaluation of melt processability of innovative dosage forms. *Int. J. Pharm.* 494, 623–642. <https://doi.org/10.1016/j.ijpharm.2015.02.009>.
- Aho, J., Edinger, M., Botker, J., Baldursdottir, S., Rantanen, J., 2016. Oscillatory Shear Rheology in Examining the Drug-Polymer Interactions Relevant in Hot Melt Extrusion. *J. Pharm. Sci.* 105, 160–167. <https://doi.org/10.1016/j.xphs.2015.11.029>.
- Baird, J.A., Olayo-Valles, R., Rinaldi, C., Taylor, L.S., 2010. Effect of molecular weight, temperature, and additives on the moisture sorption properties of polyethylene glycol. *J. Pharm. Sci.* 99, 154–168. <https://doi.org/10.1002/jps.21808>.
- Cailleaux, S., Sanchez-Ballester, N.M., Gueche, Y.A., Bataille, B., Soulaïrol, I., 2021. Fused Deposition Modeling (FDM), the new asset for the production of tailored medicines. *Journal of Controlled Release* 330, 821–841. <https://doi.org/10.1016/j.jconrel.2020.10.056>.
- Cantin, O., Siepmann, F., Danede, F., Willart, J.F., Karrout, Y., Siepmann, J., 2016. PEO hot melt extrudates for controlled drug delivery: Importance of the molecular weight. *Journal of Drug Delivery Science and Technology* 36, 130–140. <https://doi.org/10.1016/j.jddst.2016.09.003>.
- Cantin, O., 2016. PEO hot melt extrudates for controlled drug delivery (These de doctorat). Lille 2.
- Chang, Z.L., 1979. Sodium Valproate and Valproic Acid. In: Florey, K. (Ed.), *Analytical Profiles of Drug Substances*. Academic Press, pp. 529–556. [https://doi.org/10.1016/S0099-5428\(08\)60128-8](https://doi.org/10.1016/S0099-5428(08)60128-8).
- de Assis, J.M.C., Barbosa, E.J., Bezzon, V.D.N., Lourenço, F.R., Carvalho, F.M.S., Matos, J.R., Araci Bou-Chacra, N., Benmore, C.J., Byrn, S.R., Costa, F.N., de Araujo, G.L.B., 2022. Hot-melt extrudability of amorphous solid dispersions of flubendazole-copovidone: An exploratory study of the effect of drug loading and the balance of adjuvants on extrudability and dissolution. *Int. J. Pharm.* 614, 121456. <https://doi.org/10.1016/j.ijpharm.2022.121456>.
- dos Santos, J., Balbinot, G. de S., Buchner, S., Collares, F.M., Windbergs, M., Deon, M., Beck, R.C.R., 2022. 3D printed matrix solid forms: Can the drug solubility and dose customisation affect their controlled release behaviour? *Int. J. Pharm.* X 5, 100153. DOI: 10.1016/j.ijpx.2022.100153.
- Duranović, M., Madzarević, M., Ivković, B., Ibric, S., Cvijic, S., 2021. The evaluation of the effect of different superdisintegrants on the drug release from FDM 3D printed tablets through different applied strategies: In vitro-in silico assessment. *Int. J. Pharm.* <https://doi.org/10.1016/j.ijpharm.2021.121194>.
- Easyprep Pédiatrie, n.d. URL <https://www.easypreppediatrie.fr/principes-actifs/sodium-valproate-depakine/> (accessed 12.10.24).
- EMA, 2016. Reflection paper on the dissolution specification for generic oral immediate release products.
- Eu, Ph., 2024. accessed 9.8.23 European Pharmacopoeia 11.5 [WWW Document]. 11 (5). <https://pheur.edqm.eu/app/11-5/search/>.
- Goyanes, A., Robles Martinez, P., Buanz, A., Basit, A.W., Gaisford, S., 2015. Effect of geometry on drug release from 3D printed tablets. *International Journal of Pharmaceutics*, The potential for 2D and 3D Printing to Pharmaceutical Development 494, 657–663. DOI: 10.1016/j.ijpharm.2015.04.069.
- Hess, F., Kipping, T., Weitschies, W., Krause, J., 2024. Understanding the Interaction of Thermal, Rheological, and Mechanical Parameters Critical for the Processability of Polyvinyl Alcohol-Based Systems during Hot Melt Extrusion. *Pharmaceutics* 16, 472. <https://doi.org/10.3390/pharmaceutics16040472>.
- Hoffmann, L., Breitzkreutz, J., Quodbach, J., 2022. Fused Deposition Modeling (FDM) 3D Printing of the Thermo-Sensitive Peptidomimetic Drug Enalapril Maleate. *Pharmaceutics* 14, 2411. <https://doi.org/10.3390/pharmaceutics14112411>.
- Hoffmann, L., Breitzkreutz, J., Quodbach, J., 2023. Investigation of the degradation and in-situ amorphization of the enantiomeric drug escitalopram oxalate during Fused Deposition Modeling (FDM) 3D printing. *European Journal of Pharmaceutical Sciences* 185, 106423. <https://doi.org/10.1016/j.ejps.2023.106423>.
- Isreb, A., Baj, K., Wojsz, M., Isreb, M., Peak, M., Alhnan, M.A., 2019. 3D printed oral theophylline doses with innovative 'radiator-like' design: Impact of polyethylene oxide (PEO) molecular weight. *International Journal of Pharmaceutics* 564, 98–105. <https://doi.org/10.1016/j.ijpharm.2019.04.017>.
- Kimura, S., Ishikawa, T., Iwao, Y., Itai, S., Kondo, H., 2019. Fabrication of Zero-Order Sustained-Release Floating Tablets via Fused Depositing Modeling 3D Printer. *Chem. Pharm. Bull.* 67, 992–999. <https://doi.org/10.1248/cpb.c19-00290>.
- Kotsybar, J., Hakeem, S., Zhang, L., Jiang, W., 2023. Global harmonization of immediate-release solid oral drug product bioequivalence recommendations and the impact on generic drug development. *Clin. Transl. Sci.* 16, 2756–2764. <https://doi.org/10.1111/cts.13670>.
- Larsen, B.S., Kissi, E., Nogueira, L.P., Genina, N., Tho, I., 2024. Impact of drug load and polymer molecular weight on the 3D microstructure of printed tablets. *European Journal of Pharmaceutical Sciences* 192, 106619. <https://doi.org/10.1016/j.ejps.2023.106619>.
- Linares, V., Galdón, E., Casas, M., Caraballo, I., 2021. Critical points for predicting 3D printable filaments behaviour. *Journal of Drug Delivery Science and Technology* 66, 102933. <https://doi.org/10.1016/j.jddst.2021.102933>.
- Liu, X., Wang, T., Chow, L.C., Yang, M., Mitchell, J.W., 2014. Effects of Inorganic Fillers on the Thermal and Mechanical Properties of Poly(lactic acid). *Int. J. Polym. Sci.* 2014, 827028. <https://doi.org/10.1155/2014/827028>.
- Ma, L., Deng, L., Chen, J., 2014. Applications of poly(ethylene oxide) in controlled release tablet systems: a review. *Drug Dev. Ind. Pharm.* 40, 845–851. <https://doi.org/10.3109/03639045.2013.831438>.

- Melocchi, A., Parietti, F., Maroni, A., Foppoli, A., Gazzaniga, A., Zema, L., 2016. Hot-melt extruded filaments based on pharmaceutical grade polymers for 3D printing by fused deposition modeling. *International Journal of Pharmaceutics* 509, 255–263. <https://doi.org/10.1016/j.ijpharm.2016.05.036>.
- Mfoafo, K.A., Omidian, M., Bertol, C.D., Omid, Y., Omidian, H., 2021. Neonatal and pediatric oral drug delivery: Hopes and hurdles. *International Journal of Pharmaceutics* 597, 120296. <https://doi.org/10.1016/j.ijpharm.2021.120296>.
- Mora-Castaño, G., Millán-Jiménez, M., Linares, V., Caraballo, I., 2022. Assessment of the Extrusion Process and Printability of Suspension-Type Drug-Loaded Affinisol™ Filaments for 3D Printing. *Pharmaceutics* 14, 871. <https://doi.org/10.3390/pharmaceutics14040871>.
- Petrusevski, G., Naumov, P., Jovanovski, G., Bogoeva-Gaceva, G., Ng, S.W., 2008. Solid-state forms of sodium valproate, active component of the anticonvulsant drug epilim. *ChemMedChem* 3, 1377–1386. <https://doi.org/10.1002/cmdc.200800112>.
- Phachamud, T., Mueannoorn, W., Tuntarawongsa, S., Chitrattha, S., 2010. Preparation of Coated Valproic Acid and Sodium Valproate Sustained-release Matrix Tablets. *Indian J Pharm Sci* 72, 173–183. <https://doi.org/10.4103/0250-474X.65026>.
- Prasad, E., Islam, M., Goodwin, D.J., Megarry, A.J., Halbert, G.W., Florence, A.J., Robertson, J., 2019. Development of a Hot-Melt Extrusion (HME) process to produce drug loaded Affinisol™ 15LV filaments for Fused Filament Fabrication (FFF) 3D printing. *Additive Manufacturing*.
- Quodbach, J., Bogdahn, M., Breikreutz, J., Chamberlain, R., Eggenreich, K., Elia, A.G., Gottschalk, N., Gunkel-Grabole, G., Hoffmann, L., Kapote, D., Kipping, T., Klinken, S., Loose, F., Marquetant, T., Windolf, H., Geißler, S., Spitz, T., 2022. Quality of FDM 3D Printed Medicines for Pediatrics: Considerations for Formulation Development, Filament Extrusion, Printing Process and Printer Design. *Ther Innov Regul Sci* 56, 910–928. <https://doi.org/10.1007/s43441-021-00354-0>.
- Roulon, S., Soulaïrol, I., Lavastre, V., Payre, N., Cazes, M., Delbreilh, L., Alié, J., 2021. Production of Reproducible Filament Batches for the Fabrication of 3D Printed Oral Forms. *Pharmaceutics* 13, 472. <https://doi.org/10.3390/pharmaceutics13040472>.
- Sadia, M., Sośnicka, A., Arafat, B., Isreb, A., Ahmed, W., Kelarakis, A., Alhnan, M.A., 2016. Adaptation of pharmaceutical excipients to FDM 3D printing for the fabrication of patient-tailored immediate release tablets. *Int J Pharm* 513, 659–668. <https://doi.org/10.1016/j.ijpharm.2016.09.050>.
- Samaro, A., Janssens, P., Vanhoorne, V., Van Renterghem, J., Eeckhout, M., Cardon, L., De Beer, T., Vervaeke, C., 2020. Screening of pharmaceutical polymers for extrusion-Based Additive Manufacturing of patient-tailored tablets. *International Journal of Pharmaceutics* 586, 119591. <https://doi.org/10.1016/j.ijpharm.2020.119591>.
- Teixeira, L.R., Sinisterra, R.D., Vieira, R.P., Scarlatelli-Lima, A., Moraes, M.F.D., Doretto, M.C., Denadai, A.M., Beraldo, H., 2006. An Inclusion Compound of the Anticonvulsant Sodium Valproate into α -Cyclodextrin: Physico-Chemical Characterization. *J Incl Phenom Macrocycl Chem* 54, 133–138. <https://doi.org/10.1007/s10847-005-5817-y>.
- Tidau, M., Kwade, A., Finke, J.H., 2019. Influence of High, Disperse API Load on Properties along the Fused-Layer Modeling Process Chain of Solid Dosage Forms. *Pharmaceutics* 11, 194. <https://doi.org/10.3390/pharmaceutics11040194>.
- Verreck, G., Decorte, A., Heymans, K., Adriaensen, J., Cleeren, D., Jacobs, A., Liu, D., Tomasko, D., Arien, A., Peeters, J., Rombaut, P., Van den Mooter, G., Brewster, M.E., 2005. The effect of pressurized carbon dioxide as a temporary plasticizer and foaming agent on the hot stage extrusion process and extrudate properties of solid dispersions of itraconazole with PVP-VA 64. *Eur J Pharm Sci* 26, 349–358. <https://doi.org/10.1016/j.ejps.2005.07.006>.
- WHO, 2022. URL https://www.cdc.gov/growthcharts/who_charts.htm (accessed 11.22.23).
- Xie, M., Chen, J., Li, H., Li, M., 2010. Influence of poly(ethylene glycol)-containing additives on the sliding wear of ultrahigh molecular weight polyethylene/polypropylene blend. *Wear* 268, 730–736. <https://doi.org/10.1016/j.wear.2009.11.021>.
- Xu, P., Li, J., Meda, A., Osei-Yeboah, F., Peterson, M.L., Repka, M., Zhan, X., 2020. Development of a quantitative method to evaluate the printability of filaments for fused deposition modeling 3D printing. *International Journal of Pharmaceutics* 588, 119760. <https://doi.org/10.1016/j.ijpharm.2020.119760>.
- Yu, Y., Cheng, Y., Ren, J., Cao, E., Fu, X., Guo, W., 2015. Plasticizing effect of poly(ethylene glycol)s with different molecular weights in poly(lactic acid)/starch blends. *Journal of Applied Polymer Science* 132. <https://doi.org/10.1002/app.41808>.
- Yu, J., Shan, X., Chen, S., Sun, X., Song, P., Zhao, R., Hu, L., 2020. Preparation and evaluation of novel multi-channel orally disintegrating tablets. *European Journal of Pharmaceutical Sciences* 142, 105108. <https://doi.org/10.1016/j.ejps.2019.105108>.
- Zhang, J., Xu, P., Vo, A.Q., Bandari, S., Yang, F., Durig, T., Repka, M.A., 2019. Development and evaluation of pharmaceutical 3D printability for hot melt extruded cellulose-based filaments. *J Drug Deliv Sci Technol* 52, 292–302. <https://doi.org/10.1016/j.jddst.2019.04.043>.